

06
Effect of substrate misorientation on the properties of *p*-HEMT GaAs-based nanoheterostructures formed during MOCVD epitaxy

© P.B. Boldyrevskii,¹ D.O. Filatov,¹ V.A. Belyakov,¹ A.P. Gorshkov,¹ I.V. Makartsev,¹ A.V. Nezhdanov,¹ M.V. Revin,¹ A.D. Filatov,¹ P.A. Junin²

¹Lobachevsky State University,
Nizhny Novgorod, Russia

²Institute of Physics of Microstructures, Russian Academy of Sciences,
Nizhny Novgorod, Russia
e-mail: bpavel2@rambler.ru

Received May 23, 2022

Revised June 21, 2022

Accepted June 22, 2022

As one of the approaches to improve *p*-HEMT, we studied the effect of misorientation of GaAs substrates on the surface morphology, structure, and electrical properties of pseudomorphic heterostructures, as well as the parameters of transistors based on them. In a single technological cycle, heterostructures were formed on vicinal substrates with (100) orientation and misoriented by 2° to (110) by the method of MOCVD (MOCVD) in a single technological cycle. It has been established that on misoriented substrates, the growth of structurally consistent and stressed epitaxial layers occurs according to a layered-step mechanism with the formation of macrosteps. On vicinal substrates, the formation of monatomic growth steps was observed. The comparative characteristics of *p*-HEMT obtained using two types of substrates are considered.

Keywords: GaAs/InGaAs/GaAlAs heterostructures, MOCVD epitaxy, *p*-HEMT, substrate misorientation, comparative characteristics of structures and *p*-HEMT based on them.

DOI: 10.21883/TP.2022.10.54363.143-22

Introduction

Pseudomorphic HEMTs (pseudomorphic high electron mobility transistor, *p*-HEMT) are one of the promising active elements of microwave microelectronics. At present, transistors based on InGaAs/GaAlAs/GaAs heterostructures on GaAs substrates reach operating frequencies of up to 200 GHz [1]. Despite the fact that the main technological methods for manufacturing *p*-HEMTs are known and have industrial application, studies aimed at optimizing the design and technological parameters of transistors in order to increase the speed and to reduce the noise of electronic devices is of interest. Along with molecular beam epitaxy (MBE) the gas-phase epitaxy using organometallic compounds and hydrides as precursors materials (MGE/MOCVD) is the main technological process for the formation of nanoheterostructures of semiconductor compounds A₃B₅ [2]. To grow *p*-HEMT nanoheterostructures in pilot production, one usually uses either singular GaAs substrates with an exact crystallographic orientation (100) or GaAs substrates misoriented by 2° to (110) (hereinafter, as (100) + 2°). It is known that the direction and angle of misorientation of the substrate affect the growth mechanism and the crystal structure of lattice-matched and strained epitaxial layers (EL) [3]. Papers [4,5] present the results of studies of the substrate misorientation effect on the properties of InGaAs/InAlAs heterostructures grown by the MBE method and the characteristics of metamorphic HEMTs based on them. It is shown that it is possi-

ble to increase the concentration of the two-dimensional electron gas by 40%, and a shift of the peaks of the photoluminescence spectra towards photon lower energies is revealed for the case of a misoriented substrate. However, there are no data available in the known publications on the systematic study of the substrate misorientation effect on the MOCVD properties of InGaAs/GaAlAs/GaAs nanoheterostructures and transistors based on them. The task of this paper is a comparative study of the surface morphology, the degree of perfection of the crystal structure, and the electrical properties of pseudomorphic HEMT nanoheterostructures formed during MOCVD epitaxy on GaAs substrates with orientation (100) and (100) + 2°.

1. Experimental part

Epitaxial growth of semiconductor heterolayers was carried out on a modernized Epiquip VP502-RP setup equipped with a horizontal reaction chamber and induction heating of a rotating disc substrate holder. The rotation speed ~ 60 rpm [6] close to optimal for the given epitaxial system was maintained. We used standard substrates of semi-insulating GaAs produced by AXT with a diameter of 50 mm and crystallographic orientation (001) and misoriented by 2° in direction (110). As initial organometallic compounds (OMCs) for epitaxy of GaAs and ternary solid solutions AlGaAs and InGaAs, Trimethylgallium (TMG) Ga(CH₃)₃, trimethylaluminum (TMA) Al(CH₃)₃,

and trimethylindium (TMI) $\text{In}(\text{CH}_3)_3$ were used respectively, and as As source arsine AsH_3 was used. The excess of the AsH_3 concentration in the gas mixture flow over the OMC concentration was ~ 40 . Before starting the deposition process, the substrates were annealed in the reaction chamber at an epitaxy temperature of 620°C in a carrier gas atmosphere (hydrogen H_2) and AsH_3 for 5 min. Experimental samples were obtained at a total reduced pressure of the gaseous medium in the reaction chamber $p = 10^4$ Pa and an epitaxial growth rate of ≈ 0.5 nm/s, which corresponds to the main modes for device structures producing. EL of solid solutions were grown on the surface of GaAs buffer layers $d \approx 150$ nm thick. To obtain the required electron concentration in the *n*-type EL, doping with silicon was carried out during epitaxy by thermal decomposition of silane (SiH_4) in the deposition zone. At each stage of the studies a single technological cycle was carried out for the formation of a series of two samples differing only in the orientation of the substrates; (100) and (100) + 2° , respectively. The EL thicknesses were measured using a Talysurf CCI 2000 interferometer. The measurement error of the EL thickness did not exceed 1.0 nm. The overall crystalline structural perfection of the EL and the composition of the solid solutions were determined by double-crystal X-ray diffractometry on the Bruker D8 Discover diffractometer. The rocking curves near reflection (004) were recorded with a round collimator forming a beam with a diameter of ≈ 1 mm, in symmetric and grazing incidence geometry, which ensures the appropriate extinction depth. The measurement error of the diffraction angle was $\sim 0.0005^\circ$. To study the surface morphology of homo- and heteroepitaxial layers, we used atomic force microscopy (AFM) in the semi-contact mode [7]. The studies were carried out at room temperature under atmospheric conditions on the NTegra setup (manufacturer — company NT-MDT, Russia) with a Smena A scanning head. Silicon AFM probes NSG-11 manufactured by NT-MDT with a probe tip curvature radius of $R_p \approx 10$ nm were used. The relative error of coordinates measurement in the plane of the sample surface x, y in the range $1 \mu\text{m} < x, y < 100 \mu\text{m}$ was maximum 5%, the relative error in measuring the surface height (coordinate z) in the range $z < 10$ nm was $< 10\%$. The electrical and physical parameters of the samples were determined from the measurements of the Hall effect and electrical conductivity at temperatures of 77 and 300 K. The layer density of electrons and doping profiles were estimated from the measurements of the capacitance-voltage (CV) characteristics of the Schottky barrier formed by a mercury probe on the surface of EL. The field mobility of a two-dimensional electron gas (DEG) in the *p*-HEMT channel was determined from the measurements of the CV characteristics and specific conductivity at a frequency of 1 mHz.

Photoluminescence (PL) spectra were measured at 77 and 300 K using the Acton Spectra Pro 500i lattice

n^+ -GaAs (<i>contact layer</i>), $d = 60$ nm
GaAs (<i>gate undoped layer</i>), $d = 4$ nm
$\text{Al}_{0.29}\text{Ga}_{0.71}\text{As}$ (<i>upper barrier layer</i>), $d = 2$ nm
n^+ - $\text{Al}_{0.29}\text{Ga}_{0.71}\text{As}$, $d = 15$ nm, $n = 4-5 \cdot 10^{18} \text{ cm}^{-3}$
$\text{Al}_{0.29}\text{Ga}_{0.71}\text{As}$ (<i>spacer</i>), $d = 2$ nm
GaAs (<i>smoothing layer</i>), $d = 1$ nm
$\text{In}_{0.21}\text{Ga}_{0.79}\text{As}$ (<i>channel</i>), $d = 14$ nm
GaAs (<i>smoothing layer</i>), $d = 1$ nm
$\text{Al}_{0.29}\text{Ga}_{0.71}\text{As}$ (<i>barrier layer</i>), $d = 50$ nm
GaAs (<i>buffer</i>), $d = 350$ nm, $n = 1-2 \cdot 10^{14} \text{ cm}^{-3}$
Substrate GaAs (100) и (100 + 2°)

Figure 1. Schematic representation of *p*-HEMT nanoheterostructure.

monochromator equipped with the Acton ID 442A InGaAs photodetector with modulated photoexcitation (modulation frequency 180 Hz) and synchronous detection using the Stanford Research SR-810 digital synchronous detector. Photoexcitation was carried out by an unfocused radiation of the semiconductor laser with a wavelength of 472 nm and a power of 1.5 W.

A schematic representation of the structure of the studied test *p*-HEMT heterostructures grown by the MOCVD method in a single technological cycle is shown in Fig. 1.

In the studied samples there are no delta-doped silicon layers [8], which make it possible to increase the concentration of two-dimensional electron gas in basic heterostructures, since one should expect a decreased manifestation of the misorientation effect in the presence of such layers.

2. Results and discussion

According to the results of the X-ray diffraction studies of specially grown GaAs ESs and $\text{Al}_{0.29}\text{Ga}_{0.71}\text{As}/\text{GaAs}$ ($d = 150$ nm) heterostructures, no significant difference was found in the rocking curve widths for samples on the substrates of both types, which amounted to ~ 0.004 and ~ 0.005 near the reflection (004), respectively. The presented values of the rocking curve widths indicate a high structural quality of EL.

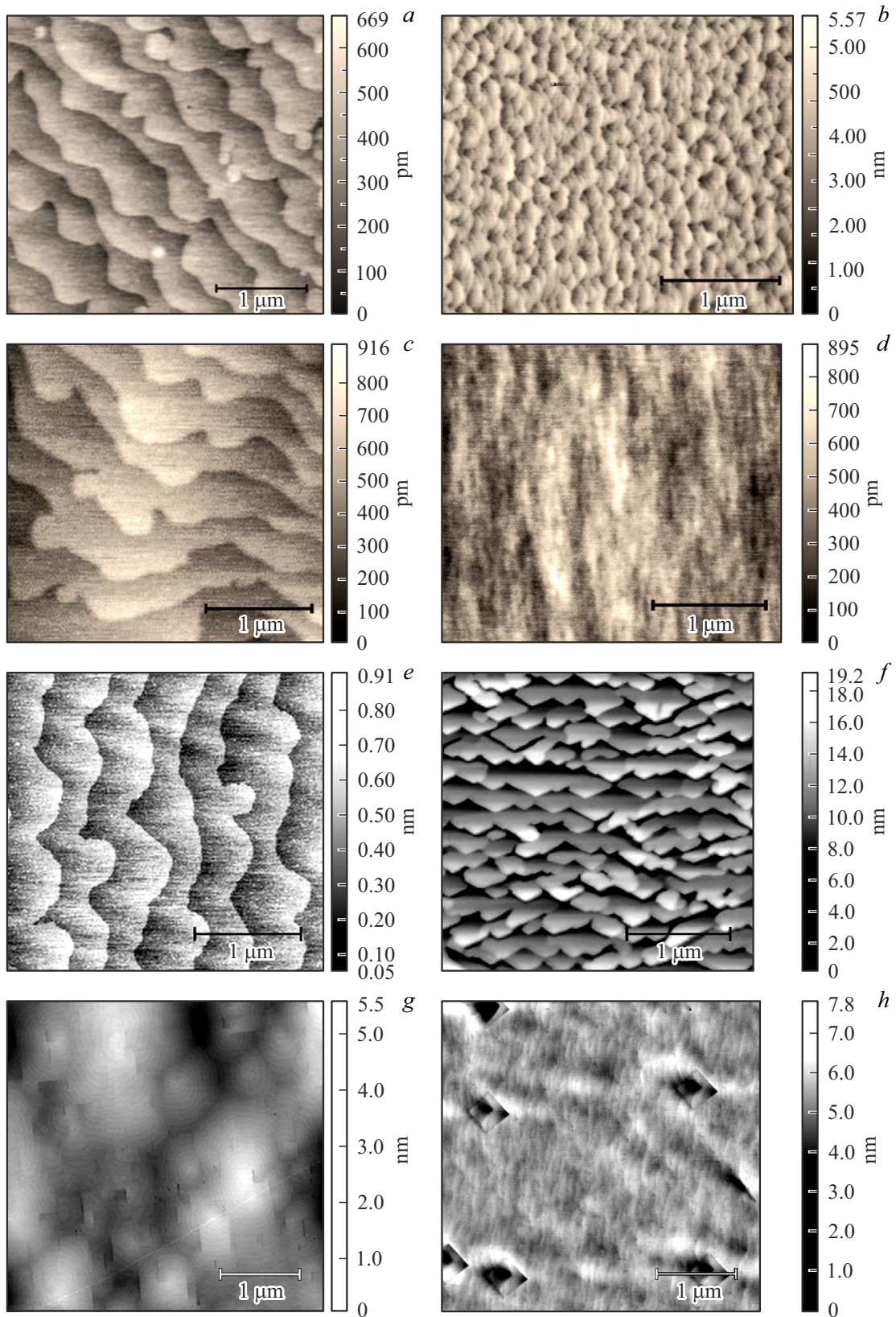


Figure 2. AFM images of the surface of AlGaAs/InGaAs/GaAs structures at different growth stages: *a, b* — initial stages of growth of the GaAs buffer layer ($t_g = 30$ s); *c, d* — surface of the GaAs buffer layer; *e, f* — surface of the InGaAs/GaAs layer; *g, h* — surface of the AlGaAs/InGaAs/GaAs layer. Substrate orientation: *a, c, e, g* — (001); *b, d, f, h* — (001) + 2°.

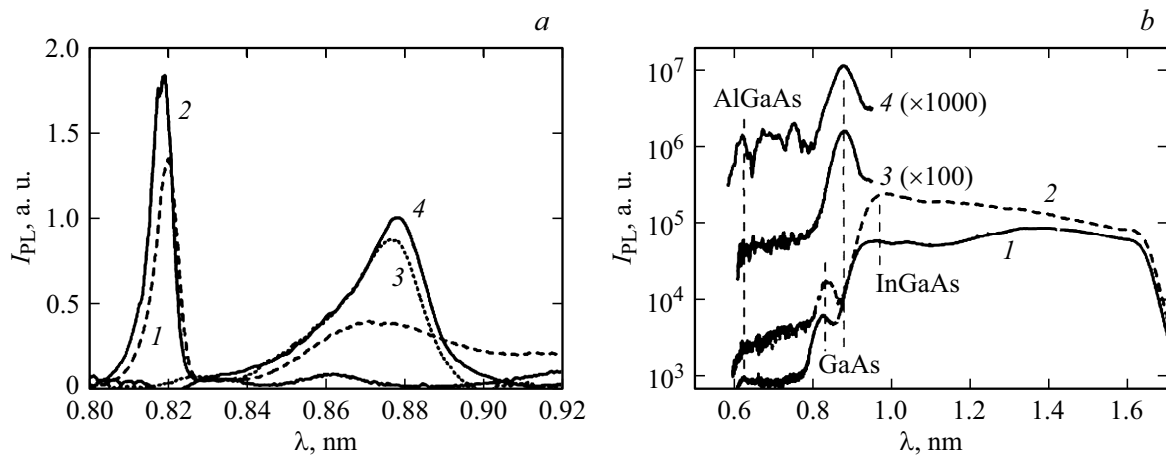


Figure 3. PL spectra: *a* — GaAs buffer layer; *b* — AlGaAs/InGaAs/GaAs structure. Substrate orientation: 1, 3 — (001) + 2°; 2, 4 — (001). *T*, K: 1, 2 — 77; 3, 4 — 300.

Fig. 2 shows the AFM images of the EL morphology during the sequential formation of the heterostructure.

On the surface of ELs grown on misoriented substrates, a regular system of periodic growth steps is observed, which indicates a layered-step mechanism of growth with the formation of macrosteps [9,10]. On GaAs (100) substrates the formation of monatomic growth steps is observed (Fig. 2, *a*). This indicates that in reality the surface planes of the used substrates did not coincide exactly with the singular face (100) of GaAs, but were misoriented with respect to it by a small amount $\arctg(h/L) \sim 0.34^\circ$. Here $L \sim 0.5 \mu\text{m}$ is the average period of monatomic growth steps (determined from the AFM data in Fig. 2), $h = a/2$ is a monatomic step height on the GaAs surface (100), $a \sim 0.565 \text{ nm}$ is the GaAs lattice constant. In connection with the foregoing, we will further call the substrates that formally have orientation (001) as vicinal ones.

Structural defects in the form of faceted pits are observed on the surface of AlGaAs/InGaAs/GaAs heterostructures (Fig. 2, *h*), the appearance of them may be associated with the local disruption of epitaxial growth as a result of slower elimination of methyl radicals — $-\text{CH}_3$ from aluminum atoms than from gallium atoms, at the edges of growth macrosteps [11].

The surface morphology of the layers of InGaAs solid solutions predominantly repeats the morphology of the underlying GaAs layers. InGaAs ELs of this composition have a thickness less than the critical one (Fig. 1), at which the formation of misfit dislocations, stacking faults and other distortions of the crystal lattice occur as a result of relaxation of the resulting mechanical stresses, which leads to a more developed surface relief [9,12]. The misorientation of the substrate leads to a step-layer mechanism of EL growth. A distinctive feature of this growth mechanism in MOSVD (unlike, for example, MBE) is the presence of a gaseous atmosphere in the reactor, while the chemisorption of hydrogen atoms and incompletely split

products of the thermal decomposition of OMC leads to the inhibition of the movement of the edges of monatomic growth steps and stimulates their aggregation into the echelons of steps followed by the formation of growth macrosteps.

Figure 3 shows the PL spectra of test samples, which are GaAs ELs, similar in parameters and growth modes to GaAs buffer layers in *p*-HEMT structures and AlGaAs/InGaAs/GaAs structures grown on vicinal and misoriented substrates. The PL spectra of the GaAs buffer layer (Fig. 3) dominate the peaks of GaAs edge PL at $\lambda \sim 0.82 \mu\text{m}$ (77 K) and $\sim 0.87 \mu\text{m}$ (300 K). The edge PL intensity of the GaAs layer grown on substrate (100) was by $\sim 40\%$ higher than that of the layer grown on substrate (100) substrate + 2° — both at 77, and at 300 K.

In addition to GaAs edge PL, the PL spectra at 77 K exhibit broad peaks in the $\lambda \sim 0.86\text{--}0.88 \mu\text{m}$ region, which are presumably associated with deep levels in GaAs [13]. The intensity of these peaks for EL GaAs grown on a misoriented substrate significantly exceeds the intensity of the corresponding peak in EL GaAs grown on a vicinal substrate (compare curves 1 and 2 in Fig. 3, *a*). This may be associated with an increased concentration of optically active deep centers in the EL GaAs grown on the misoriented substrate due to segregation and the impurities capture by growth macrosteps.

The PL spectra of the AlGaAs/InGaAs/GaAs structures (Fig. 3, *b*) at 77 K exhibit PL bands with a high-energy edge near $\lambda \sim 0.62 \mu\text{m}$ associated with interband radiative recombination in AlGaAs. The value of $\lambda \sim 0.62 \mu\text{m}$ at 77 K corresponds to the Al concentration in $\text{Al}_x\text{Ga}_{1-x}\text{As}$. The PL peaks at $\lambda \sim 0.83 \mu\text{m}$ (77 K) and $\sim 0.87 \mu\text{m}$ (300 K) are related to the edge PL in the GaAs buffer layer. The PL band in the spectral region $\lambda = 0.9\text{--}1.6 \mu\text{m}$ (77 K) is associated with impurity PL in AlGaAs with the participation of DX centers [14]. The short-wavelength shoulder of this band (maximum at $\lambda \sim 0.96 \mu\text{m}$) is associated with interband radiative recombination between the

Table 1. Electrophysical parameters of EL GaAs

Parameter	Substrate GaAs (100) + 2°		Substrate GaAs (100)	
	Concentration SiH ₄ in gas mixture flow, mmol/min	0.01	0.12	0.01
Mobility, cm ² /B · c at 300 K	5600* 4950**	3500* 3100**	5400* 5350**	3200* 3300**
Mobility, cm ² /(V · s) at 77 K	19 000* 18 000**	5300* 5000**	23 000* 23 000**	5150* 5100**
Concentration, <i>n</i> , cm ⁻³	1.0 · 10 ¹⁶ * 1.2 · 10 ¹⁶ **	1.7 · 10 ¹⁷ * 1.7 · 10 ¹⁷ **	0.8 · 10 ¹⁶ * 0.85 · 10 ¹⁶ **	1.0 · 10 ¹⁷ * 1.1 · 10 ¹⁷ **

Note. * — direction of current along the base cut of the substrate (for 100 + 2° — along the macrosteps), ** — turn by 90°.

Table 2. Static and UHF parameters of *p*-HEMT based on heterostructures formed using (100) and (100) + 2 GaAs substrates

Parameter	GaAs (100) + 2° substrate	GaAs (100) substrate
DEG mobility, cm ² /(V · s) (300 K)	7900	8580
DEG concentration, 10 ¹² sm ⁻²	1.67	1.65
Slope, <i>g</i> , mSm/mm	440	450
Gain <i>G</i> _{max} (measurements at frequency <i>f</i> = 10 GHz), dB	18.0	18.5
Noise coefficient, NF (measurements in the frequency range 1–40 GHz), dB	1.9 · 2.5	1.4 · 2.2

ground quantum states of electrons and holes in the InGaAs layer.

In general, the above results allow us to conclude that the structural and, as a consequence, the optical properties of structures grown on vicinal substrates are higher than those of misoriented ones.

As follows from the data presented in Table 1, for the structures grown on substrate ((100) + 2°), there is a pronounced anisotropy of the Hall mobility of electrons, which is maximum when the direction of current carrier transfer is along the edges of the macrosteps.

Some increasing of the doping level of EL when using GaAs (100) + 2° substrates is associated with increased rate of capture of the (Si) dopant by macrosteps.

Table 2 lists the static and UHF parameters of *p*-HEMT with a gate length of *L* = 70 nm. The *p*-HEMT channels on heterostructures with GaAs (100) + 2° substrates are oriented along the edges of the macrosteps.

In general, the parameters of *p*-HEMTs formed on the basis of heterostructures obtained using vicinal substrates GaAs (100) exceed the parameters of devices developed on the basis of heterostructures with substrates GaAs (100) + 2°. The achievement of the minimum noise factor on heterostructures with substrates GaAs (100) seems to be the most important result.

Conclusion

The results of this paper show that the use of MOCVD epitaxy to create *p*-HEMT nanoheterostructures is quite promising, and at the same time it can have a number of features associated with the effect of misorientation of GaAs substrates. In the case of using GaAs substrates misoriented by 2° to (110), it is necessary to take into account the features of layered-step epitaxial growth with the formation of macrosteps. The main features are the observed anisotropy of the electron mobility, while the arrangement of the transistor channels should be along the edges of the macrosteps. This feature makes it necessary to carry out appropriate additional measurements and studies in comparison with technologies where vicinal substrates GaAs (100) are used. The performed studies showed that certain parameters of *p*-HEMT on heterostructures grown on vicinal substrates GaAs (100) exceed the parameters of *p*-HEMT on misoriented substrates. Thus, we can conclude that the use of vicinal substrates GaAs (100) in the technologies under consideration is more promising.

Acknowledgments

The measurements of FL spectra were performed using the equipment of the Center of Shared Use of the Science & Education Center Nanostructure Solid-State Physics of the Lobachevsky State University of Nizhny Novgorod.

Conflict of interest

The authors declare that they have no conflict of interest.

References

- [1] D.-H. Kim, J.A. del Alamo. *IEEE Electron. Dev. Lett.*, **31** (81), 80–806 (2010).
- [2] S. Irvine, P. Capper, S. Kasap, A. Willoughby. *Metalorganic Vapor Phase Epitaxy (MOVPE): Growth, Materials Properties and Applications* (Wiley, Hoboken, 2019), 424 p.
- [3] R.M. Biefeld, D.D. Koleske, J.G. Cederberg. *The Science and Practice of Metal-Organic Vapor Phase Epitaxy (MOVPE) // Handbook of Crystal Growth: Thin Films and Epitaxy: 2nd Ed.*—Ed. T.F. Kuech (Elsevier, Amsterdam, 2015), p. 95–160.
- [4] P.V. Seredin, A.S. Lenshin, A.V. Fedyukin, I.N. Arsentiev, A.V. Jabotinsky, D.N. Nikolaev, H. Leiste, M. Rinke. *Semiconductors*, **52** (1), 417 (2018). DOI: 10.21883/FTP.2018.01.45329.8565
- [5] V.A. Kulbachinskii, L.N. Oveshnikov, R.A. Lunin, N.A. Yuzeeva, G.B. Galiev, E.A. Klimov, S.S. Pushkarev, P.P. Maltsev. *Semiconductors*, **49** (7), P. 942, (2015).
- [6] P.B. Boldyrevskii, D.O. Filatov, I.A. Kazantseva, M.V. Revin, D.S. Smotrin, P.A. Yunin. *Tech. Phys.*, **63** (2), 211 (2018). DOI: 10.21883/0000000000
- [7] S.N. Magonov. *Surface Analysis with STM and AFM. Experimental and Theoretical Aspects of Image Analysis* (Wiley-VCH, Weinheim, 1996), 323 p.
- [8] *Pseudomorphic HEMT Technology and Applications*, ed. by R.L. Ross, S.P. Svensson, P. Lugli (Springer, Berlin–Heidelberg, 1996), 320 p.
- [9] P.B. Boldyrevskii, D.O. Filatov, I.A. Kazantseva, M.V. Revin, P.A. Yunin, A.D. Filatov. *Tech. Phys.*, **90** (5), 791 (2020). DOI: 10.21883/0000000000
- [10] R. Nötzel, K.H. Ploog. *Adv. Mater.*, **5** (22), 22–29 (1993).
- [11] S. Irvine, P. Capper, S. Kasap, A. Willoughby. *Metalorganic Vapor Phase Epitaxy (MOVPE): Growth, Materials Properties and Applications* (Wiley, Hoboken, 2019), 424 p.
- [12] G.B. Galiev, I.S. Vasil'evskii, S.S. Pushkarev, E.A. Klimov, R.M. Imamov, P.A. Buffat, B. Dwir, E.I. Suvorova. *J. Cryst. Growth*, **366**, 55 (2013).
- [13] M.R. Brozel, G.E. Stillman. *Properties of Gallium Arsenide* (Institution Engineer. Technol., 1996), 350 p.
- [14] S. Adachi. *Properties of Aluminium Gallium Arsenide* (Institution Engineer. Technol., 1993), 325 p.